ESR Spin Trapping Studies of Free Radicals Generated from Nitrofuran Derivative Analogues of Nifurtimox by Electrochemical and *Trypanosoma cruzi* Reduction

CLAUDIO OLEA-AZAR[a,*], CAROLINA RIGOL[a], FERNANDO MENDIZABAL[b], ANTONIO MORELLO[d], JUAN DIEGO MAYA[d], CLAUDIO MONCADA[e], ELIANA CABRERA[c], ROSSANA DI MAIO[c], MERCEDES GONZÁLEZ[c] and HUGO CERECETTO[c]

[a]*Department of Inorganic and Analytical Chemistry, Faculty of Chemical and Pharmaceutical Sciences, University of Chile, P.O. Box 233, Santiago 1, Chile;* [b]*Department of Chemistry, Faculty of Sciences, University of Chile, P.O. Box 653, Santiago, Chile;* [c]*Department of Organic Chemistry, Faculty of Chemistry, University of the Republic, Montevideo, Uruguay;* [d]*Department of Molecular and Clinical Pharmacology, Faculty of Medicine, University of Chile, P.O. Box 70000, Santiago 7, Chile;* [e]*Department of Pharmacology and Toxicology, Faculty of Chemical and Pharmaceutical Sciences, University of Chile, P.O. Box 233, Santiago 1, Chile*

Electron spin resonance (ESR) spectra of radicals obtained from two analogues of the antiprotozoal drug nifurtimox by electrolytic and *Trypanosoma cruzi* reduction were analyzed. The electrochemistry of these compounds was studied using cyclic voltammetry. STO 3-21G *ab initio* and INDO molecular orbital calculations were performed to obtain the optimized geometries and spin distribution, respectively. The antioxidant effect of glutathione on the nitroheterocycle radical was evaluated. DMPO spin trapping was used to investigate the possible formation of free radicals in the trypanosome microsomal system. Nitro1 and Nitro2 nitrofuran analogues showed better antiparasitic activity than nifurtimox. Nitro2 produced oxygen redox cycling in *T. cruzi* epimastigotes. The ESR signal intensities were consistent with the trapping of either the hydroxyl radical or the Nitro2 analogue radicals. These results are in agreement with the biological observation that Nitro2 showed anti-Chagas activity by an oxidative stress mechanism.

Keywords: Nitrofuran derivatives; ROS scavenging; ESR spin trapping; Cyclic voltammetry; *T. Cruzi*; Oxidative stress

INTRODUCTION

Parasitic diseases in tropical and subtropical areas constitute a major health and economic problem. Chagas' disease, produced by several strains of *Trypanosoma cruzi*, affects approximately 24 million people from Southern California to Argentina and Chile.[1] Nifurtimox (Fig. 1) and benznidazole are currently used to treat this disease.[2] A characteristic Electron spin resonance (ESR) signal corresponding to the nitro anion radical ($R\text{-}NO_2^{\cdot}$) appears when nifurtimox is added to intact *T. cruzi* cells.[3] This and other experiments[4–6] suggest that intracellular reduction of nifurtimox followed by redox cycling, yielding $O_2^{-\cdot}$ and H_2O_2, may be the major mode of action against *T. cruzi*. However, the use of nifurtimox has the disadvantage of its side effects.[7]

Nitro compounds, especially 5-nitrofuryl derivatives, have been documented to be of great value as antiparasitic drugs. Recently, we have explored 5-nitro-2-furaldehyde derivatives to find new substances with less side effects than Nifurtimox.[8–12] We have also carried out three-dimensional quantitative structure-activity relationship (3-D QSAR) studies on the *in vitro* and *in vivo* antiparasitic activities against *T. cruzi* to establish the pharmacophore for this kind of semicarbazone derivatives.[13,14]

Other nitroheterocyclic compounds such as megazol and related nitroimidazole compounds are being tested as antichagasic drugs. Megazol has shown

*Corresponding author. E-mail: colea@uchile.cl

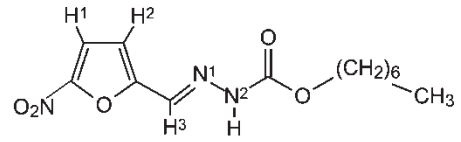

Nitro 1

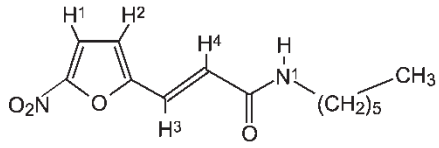

Nitro 2

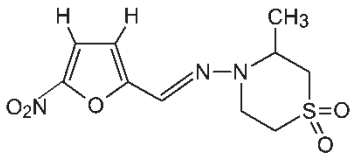

Nifurtimox

FIGURE 1 Chemical structure of the nitroheterocyclic derivatives.

antiprotozoal and antibacterial activity.[15,16] Specifically, the single-electron reduction of megazol by NADPH: cytochrome P-450 reductase, by rat liver as well as by trypanosome microsomes has been confirmed by ESR experiments.[17] Consequently, the nitro anion radical production by one-electron reduction of megazol may be the key step in the reaction mechanism.

In general, the biological effects of nitroheterocyclic compounds, especially in *T. cruzi*, are believed to involve redox cycling of these compounds and oxygen radical production, two processes in which the nitroanion radicals play an essential role.[18]

We have previously reported studies on antiprotozoal 5-nitrofurfural and 5-nitrothiophene-2-carboxaldehyde derivatives. These compounds were shown to generate nitroanion radicals, which were characterized using ESR spectroscopy.[19–20]

Here, we report electrochemical and ESR spin trapping studies of two new nitrofuran derivatives: heptyl (5-nitro-2-furylmethylidene)-1-hydrazin-2-carboxylate (Nitro 1) and N-hexyl (5-nitro-2-furyl)-3-acrylamide (Nitro 2) (Fig. 1). The formal one-electron transfer potential for the new nitroheterocyclic compounds was compared with that of Nifurtimox. From these experiments a simple relationship between the reduction potential and the biological activities was found. The anion radicals produced in the electrochemical process and in the *T. cruzi* system were characterised by ESR. In addition, the present results provided in this study support the contention that glutathione can act as a free radical scavenger with free radical species of nitrofuran derivatives (Nitro 1 and 2).

To estimate the theoretical hyperfine constants, INDO-SCF calculations were carried out. The geometry of each nitro compound in both spin-paired and free radical forms was fully optimized by the STO 3-21G *ab initio* methodology.

Finally, we measured the percentage of growth inhibition in *T. cruzi* cultures and the oxygen consumption by trypanosomes in the presence of these nitroheterocyclic compounds in order to suggest a possible underlying mechanism.

EXPERIMENTAL SECTION AND THEORETICAL METHODS

Samples

The nitrofuran derivatives were synthesized as:

Heptyl 4-(5-nitrofurfurylidene)carbazate (**Nitro1**): a mixture of 5-nitro-2-furaldehyde (1 equiv.), heptyl carbazate (1 equiv.), *p*-TsOH (*p*-toluenesulfonic acid) in catalytic amounts and toluene as solvent was stirred at room temperature until the carbonyl compound was no longer present (SiO_2, 1% Methanol in CH_2Cl_2). The resulting precipitate was collected by filtration and was crystallized from petroleum ether:EtOAc. Yellow needles (45%). ^{1}H-NMR ($CDCl_3$, 400 MHz) δ: 0.89 (t, 3H, $J = 7.1$ Hz), 1.30 (m, 8H), 1.69 (quint, 2H, $J = 6.9$ Hz), 4.24 (t, 2H, $J = 6.7$ Hz), 7.00 (d, 1H, $J = 3.8$ Hz), 7.36 (d, 1H, $J = 3.8$ Hz), 8.05 (bs, 1H), 8.50 (bs, 1H). IR ν: 3221.5, 1743.9, 1230.7, 819.8. MS m/z: 297 (M^+), 267, 182. mp(°C) 121.9–123.0 (Petroleum ether:EtOAc). *Anal.* Calcd for $C_{13}H_{19}N_3O_5$: C, 52.53; H, 6.40; N, 14.14. Found: C, 52.58; H, 6.27; N, 14.31.

N-Hexyl 3-(5-nitrofuryl)propenamide (**Nitro2**). (a) *N*-[3-(5-Nitrofuryl)propenoyl] oxysuccinimide: a mixture of 3-(5-nitrofuryl)propenoic acid[21] (0.50 g, 2.7 mmol) and *N*-hydroxysuccinimide (0.31 g, 2.7 mmol) in dry CH_2Cl_2 (10.0 ml) was stirred at 0°C (ice/water), then 1,3-dicyclohexylcarbodiimide (DCC) (0.56 g, 2.7 mmol) was added. The reaction mixture was allowed to stir for 1 h more at 0°C and for 24 h at room temperature. The solid (dicyclohexylurea) was collected by filtration, washed with CH_2Cl_2 and the filtrate concentrated under reduced pressure. The resulting solid was washed with hot ethanol:petroleum ether (1:1). Beige solid (0.34 g, 45%). ^{1}H-NMR ($CDCl_3$, 400 MHz) δ: 2.88 (s, 4H), 6.80 (d, 1H, $J = 15.9$ Hz), 6.89 (d, 1H, $J = 3.8$ Hz), 7.36 (d, 1H, $J = 3.8$ Hz), 7.62 (d, 1H, $J = 15.9$ Hz). MS m/z: 280 (M^+). mp(°C) 210.0 (d). *Anal.* Calcd for $C_{11}H_8N_2O_7$: C, 47.14; H, 2.86; N, 10.00. Found: C, 46.96; H, 2.51; N, 10.31. (b) A mixture of *N*-[3-(5-nitrofuryl)propenoyl]oxysuccinimide (1 equiv.),

hexylamine (1.2 equiv.) and dry CH_2Cl_2 as solvent was stirred at room temperature until the intermediate was not present (SiO_2, 40% EtOAc in petroleum ether). The mixture was concentrated *in vacuo* and treated with EtOAc. After work-up the residue was purified by column chromatography (SiO_2, petroleum ether:EtOAc (0 to 20%)); brown-orange solid (48%). ^{1}H-NMR ($CDCl_3$, 400 MHz) δ: 0.92 (t, 3H, $J = 6.7$ Hz), 1.34 (m, 4H), 1.58 (m, 4H), 3.41 (q, 2H, $J = 7.1$ Hz), 5.79 (bs, 1H), 6.66 (d, 1H, $J = 15.3$ Hz), 6.70 (d, 1H, $J = 3.8$ Hz), 7.34 (d, 1H, $J = 3.7$ Hz), 7.42 (d, 1H, $J = 15.3$ Hz). IR ν: 3275.5, 1655.1, 817.9. MS m/z: 266 (M^+), 249, 166. mp(°C) 102.5–104.0. *Anal.* Calcd for $C_{13}H_{18}N_2O_4$: C, 53.76; H, 6.77; N, 10.53. Found: C, 53.75; H, 6.77; N, 10.38.

Reagents

Dimethylsulfoxide (DMSO) (spectroscopy grade), glutathione (GSH), 5,5-dimethyl-1-pyrroline N-oxide (DMPO), reduced Nicotinamide Adenine Dinucleotide Phosphate (NADPH), ethylenediaminetetraacetic acid (EDTA) were obtained from Sigma Aldrich Co., St Louis, MO. Tetrabutylammonium perchlorate (TBAP) used as supporting electrolyte was obtained from Fluka.

Cyclic Voltammetry

Cyclic voltammetry was carried out using a Weenking POS 88 instrument with a Kipp Zenen BD93 recorder, in DMSO (*ca* 1.0×10^{-3} mol dm^{-3}), under a nitrogen atmosphere, with TBAP (*ca* 0.1 mol dm^{-3}), using three-electrode cells. A hanging drop mercury electrode (HDME) was used as the working electrode, a platinum wire as the auxiliary electrode, and saturated calomel (SCE) as the reference electrode. The nitroheterocyclic radicals were generated by electrolytic reduction or by the *T. cruzi* system *in situ* at room temperature.

ESR Spectroscopy

ESR spectra were recorded in the X band (9.85 GHz) using a Bruker ECS 106 spectrometer with a rectangular cavity and 50 kHz field modulation. The hyperfine splitting constants were estimated to be accurate within 0.05 G. ESR spectra of the nitroheterocyclic anion radicals were obtained in the electrolysis solution. Also, radical oxygen species were produced using a microsomal fraction (4 mg protein/ml) obtained from *T. cruzi*, in a reaction medium containing 1 mM NADPH, 1 mM EDTA and 100 mM DMPO, in 20 mM phosphate buffer, pH 7.4. The ESR spectra were simulated using the program WINEPR Simphonia 1.25 version.

Parasites

T. cruzi epimastigotes (Tulahuén strain), from our collection, were grown at 28°C in Diamond's monophasic medium as reported earlier,[22,23] with blood replaced by 4 μM hemin. Fetal calf serum was added to a final concentration of 4%. Parasites: 8×10^7 cells correspond to 1 mg protein or 12 mg of fresh weight.

Oxygen Uptake

Tulahuén strain *T. cruzi* epimastigotes were harvested by 500 *g* centrifugation, followed by washing and re-suspension in 0.05 M sodium phosphate buffer, pH 7.4, containing 0.107 M sodium chloride. Respiration measurements were carried out polarographically with a Clark N° 5331 electrode (Yellow Springs instruments) in a 53 YSI model (Simpson Electric Co.).[24] The assays were performed in a 2 ml chamber at 28°C, using 2 mg of protein. In order to evaluate redox cycling, mitochondrial respiration was inhibited with 20 μM sodium cyanide. IC_{kc50} equivalent concentration corresponds to the final concentration used in the oxygen uptake experiments. This concentration was calculated considering that the IC_{kc50} (culture growth experiments) was determined using 3×10^6 parasites/ml, equivalent to 0.0375 mg protein/ml as initial parasite mass. In the oxygen uptake experiments, 8×10^7 parasites/ml, equivalent to 1 mg protein per ml, was used.[25] In order to maintain the parasite mass-drug ratio constant in these two types of experiments, the original IC_{kc50} was corrected by this 26-fold parasite mass increase in the oxygen uptake experiments. Values are expressed as mean ± SD for three independent experiments. No effect of DMSO was observed.

Epimastigote Culture Growth Inhibition

Four to five different concentrations of each drug dissolved in DMSO were added to a suspension of 3×10^6 *T. cruzi* epimastigotes per ml (Tulahuen strain). Final concentrations in the culture growth were between 10 and 250 μM for each drug. Parasite growth was followed by nephelometry for 10 days. No toxic effect of DMSO was observed.

Culture growth constant (kc) for each drug concentration employed was calculated using the epimastigote exponential growth curve (regression coefficient > 0.97, $p < 0.05$). The slope resulting from plotting Ln of the nephelometry reading vs. time corresponds to the kc (h^{-1}). IC_{kc50} is defined as the drug concentration at which a 50% reduction of growth is obtained when compared to control. It is calculated by lineal regression analysis from the kc values obtained for each drug concentration

studied.[23] Values are expressed as mean ± SD for three independent experiments.

Theoretical Calculations

Full geometry optimizations of the nitrofuran derivatives in spin-paired and free radical forms were carried out by STO (Slater Type Orbital) 3-21G methods.[26] STO 3-21G calculations were done employing the open shell UHF option (Unrestricted Hartree- Fock). The theoretical hyperfine constants were obtained using INDO (Intermediate Neglect of Differential Overlap) approximation semiempirical methodology.[27,28]

RESULTS AND DISCUSSION

Cyclic Voltammetry

Table I lists the values of the voltammetric peaks and the anodic and cathodic currents for all compounds. All nitroheterocyclic compounds display comparable voltammetric behaviour, showing two well-defined reduction waves in DMSO.

The first wave for all compounds studied corresponds to a reversible one-electron transfer. The reverse scan showed the anodic counterpart of the reduction waves. The width of the cathodic wave at its half intensity has a relatively constant value of 60 mV. The intensity ratio ipa/ipc has a value close to one (Fig. 2). According to the standard reversibility criteria this couple corresponds to a reversible diffusion-controlled one-electron transfer. It is attributable to the reduction of R-NO_2 to $RNO_2^{-\bullet}$, a stable anion radical at room temperature. These nitrofurans exhibited lower cathodic peak potential values (Epc) than Nifurtimox, which is a well-known drug used in the therapy of Chagas' disease (Table I). Also, a good correlation between the reduction peak potential values corresponding to these nitrocompounds and the IC_{kc50} value was found (Table III).

The second cathodic peak is irreversible in the whole range of sweep rates used (50–1000 mV/s). We can attribute this wave to the production of the hydroxylamine derivative.

A third couple appears for both nitroheterocycles, being irreversible for nitro1 and quasireversible for Nitro2 in the whole sweep rate range used. A fourth quasireversible couple was only observed for Nitro2. These couples could be attributed to the reduction of the side chain carbonyl group in two steps: first, the radical carboxyl derivative, and second, the alcohol derivative product.

We evaluated the effects of GSH on the first voltammetric couple of both compounds. In this regard, the signal was proportional to the quantity of the radical present in the solution, i.e. proportional to the amount of radical produced by electrolysis. Also, it was possible to observe for both nitrocompounds (Nitro 1 and 2) that the anodic peaks decrease until practically disappeared concomitantly with the increase in GSH concentration from 0.2 to1.0 mM, and the couple become irreversible (data not shown). The explanation for this change in the peak current may be that the potential reaction of GSH with radicals lowers of amount of Nitro 1 and 2, respectively, available for voltammetric measurements.

ESR

Electrochemical reduction to the radical forms (*in situ*) in DMSO were carried out applying the potential corresponding to the first wave for the nitroheterocyclic compounds, as obtained from the CV experiments.

Interpretation of the ESR spectra by means of a simulation process has led to the determination of the coupling constants for all magnetic nuclei and is corroborated by quantum chemical calculations.

Nitro **1** was analyzed in terms of (i) one triplet due to the nitrogen of the nitro group; (ii) two doublets due to the hydrogens corresponding to the furan

TABLE I Cyclic voltammetric parameters of nitrofuran derivatives in DMSO vs. calomel electrode

Nitrofuran derivative	Couple	Epc (V)	Epa (V)	ΔEp (V)	ipa/ipc	$E_{1/2}$ (V)
Nitro 1	I	−0.823	−0.727	0.096	1.02	−0.775
	II	−1.573	–	–	–	–
	III	−2.065	–	–	–	–
	IV	−2.319	−2.132	0.187	1.50	−2.226
Nitro 2	I	−0.802	−0.713	0.089	1.01	−0.758
	II	−1.474	–	–	–	–
	III	−2.070	−1.987	0.083	1.26	−2.069
Nifurtimox	I	−0.91	−0.85	0.06	1.01	−0.88

Epc, cathodic potential vs SCE; Epa, anodic potential vs SCE; ΔEp, Epa − Epc; ipa/ipc, ratio between the anodic and cathodic intensities calculated following the Nicholson equation: $ipa/ipc = (ipa_0)/(ipc) + 0.485(ip\lambda_0)/(ipc) + 0.086$; $E_{1/2} = (Epc + Epa)/2$. For details, see Materials and Methods section.

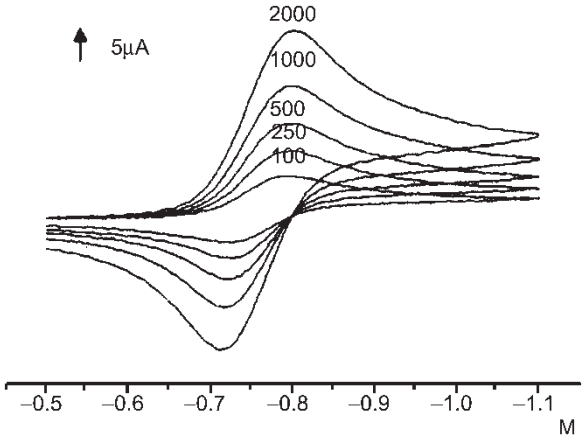

FIGURE 2 First couple of Nitro 1 in DMSO obtained at the following sweep rates: 2000, 1000, 5000, 250 and 100 mV/sec.

ring; (iii) two triplets due to the two nitrogens of the side chain and (iv) one doublet due to hydrogen 3. The hyperfine constant of hydrogen assigned to the NH group proved to be smaller than the line width; therefore, it was not observed in the experimental spectrum. These results are in agreement with our theoretical calculation that predicted a very small hyperfine constant for this atom (Fig. 3). The hyperfine constants are listed in Table II.

The ESR spectrum of nitro **2** was simulated in terms of (i) one triplet corresponding to the nitrogen nucleus of the nitro group; (ii) four doublets due to non-equivalent hydrogens 1, 2, 3 and 4; and (iii) one triplet due to the nitrogen positioned in the side chain (iv) one doublet due to hydrogen attached to the side chain nitrogen, and (v) one triplet due to the hydrogens of one methylene group (Fig. 3). The hyperfine constants are listed in Table II.

Finally, when the radical anions were formed by electrochemical reduction, 1 mM GSH was added in both solutions. The presence of GSH decreases the intensity of the signals of Nitro 1 and 2 until they eventually become undetectable (data not shown). Furthermore, to assess the type of interaction, spin trapping studies using DMPO were conducted. DMPO was added to the reaction mixture after the electrolytic generation of the Nitro 1 and 2 radical anions in the presence of 1 mM GSH. Three minutes after the addition of the spin trap typical ESR spectra of DMPO appeared for both compounds. The spectrum has four lines, with a constant of 15.10 G ($a_N = a_H$), a typical value corresponding to the trapping of GS· radical by DMPO.[29] Figure 4 shows the DMPO-GS adduct generated from Nitro 2.

ESR Evidence for Production of Free Radical Species by *T. cruzi*

As expected, the incubation of Nitro 1 with *T. cruzi* homogenates in the presence of NADPH and EDTA

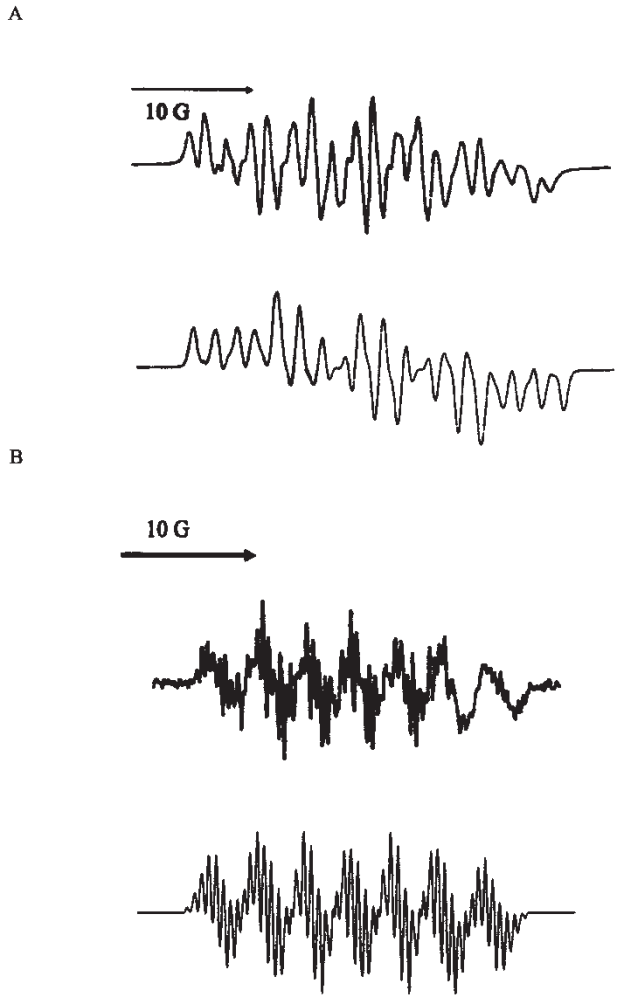

FIGURE 3 (A) ESR experimental spectrum of the radical-anion of Nitro 1 in DMSO and computer simulation of the same spectrum. Spectrometer conditions: microwave frequency 9.68 GHz microwave power 20 mW, modulation amplitude 0.2 G, scan rate 1.25 G/s, time constant 0.5 s, number of scans: 15. Spectrum was simulated using the following parameters: line width = 0.7 G, ratio Lorentzian/Gaussian = 0.8 and hyperfine constants included in Table II; (B) ESR experimental spectrum of the radical-anion of Nitro 2 in DMSO and computer simulation of the same spectrum. Spectrometer conditions: microwave frequency 9.68 GHz microwave power 20 mW, modulation amplitude 0.2 G, scan rate 1.25 G/s, time constant 0.5 s, number of scans: 15. Spectrum was simulated using the following parameters: line width = 0.1 G, ratio Lorentzian/Gaussian = 1.0 and hyperfine constants included in Table II.

did not generate the anion nitro radical. When DMPO was added in order to analyse the production of radical oxygen species, no ESR signal was detected. A weak ESR signal was observed for Nitro 2 when it was incubated in the presence of *T. cruzi* microsomes, probably attributable to Nitro 2 radical species. However, a well-resolved ESR spectrum appeared when DMPO was added to the *T. cruzi* system. The ESR signal intensity was consistent with the trapping of both the hydroxyl radical and the nitroheterocycle radical for Nitro 2, (DMPO-OH spin adduct $a_N = a_H = 14.78$ G; DMPO-Nitro 2 spin adduct $a_N = 15.21$ G, $a_H = 23.48$ G) Fig. 5.

TABLE II Experimental and theoretical hyperfine splittings (Gauss) and g values for the nitroheterocyclic anion radicals

Nitroheterocycle		*a_{H1}	a_{H2}	a_{H3}	a_{H4} [G]	a_N (NO_2)	a_{N1}	a_{N2}	a_H (NH)	a_H (CH_2)	*g* value
Nitro 1	EXP	5.20	1.35	0.68	–	6.95	2.80	1.85	–	–	2.0057
	TEOR	6.00	1.20	0.30	–	6.30	2.10	1.10	–	–	
Nitro 2	EXP	4.25	3.25	1.05	0.7	6.8	0.60	–	0.65	0.42	2.0059
	TEOR	4.80	3.50	1.10	1.00	6.40	0.50	–	0.45	0.38	

*See Fig. 1. For details, see Materials and Methods section.

These hyperfine constants are in agreement with the splitting constants of other DMPO-OH adducts and nitrogen-centered radical trapping by DMPO.[30,31] These results are in agreement with the oxygen uptake experiments, since they clearly show that only the Nitro 2 compound presents a redox cycling process similar to nifurtimox (Table III). On the other hand, Nitro 1-induced growth inhibition of *T. cruzi* occurs at concentrations that do not stimulate hidroxyl radical generation.

Since the drugs employed in this study are of lipophilic character, they are rapidly and almost completely absorbed by the parasites. Thus, the relationship between the amount of drug and the number of parasites becomes important. When the IC_{kc50} and the IC_{kc50} equivalent concentrations are expressed as nmol of drug per milligram of parasite protein, the values became similar (Table III); and in this way, it was possible to validate the comparison between the inhibition of culture growth and the parasite respiration data. The drug effect upon respiration (Table III) is shown at a dose equal to the concentration at which the culture growth is inhibited by fifty percent. Additionally, other experiments were done (data not shown) using drug doses from 0.3 to 3 times the IC_{kc50} equivalent concentration. These experiments showed that the respiratory effect was proportional to the drug concentration in the range of doses employed.

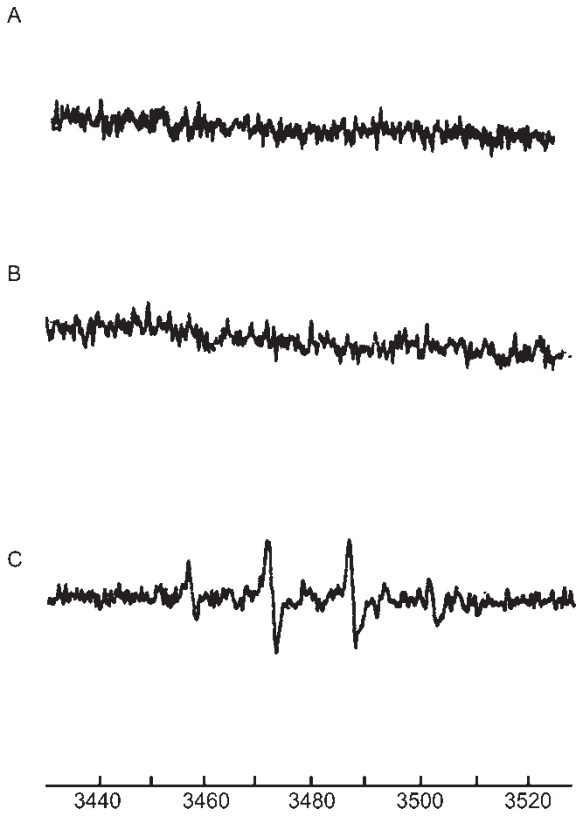

FIGURE 4 DMPO-GS adduct obtained after electrolysis of Nitro 2 in DMSO in the presence of GSH and DMPO. (A) DMPO (100 mM) in the presence of GSH (1 mM); (B) GSH (1 mM) added to Nitro2 (1 mM) after electrolysis; (C) DMPO (100 mM) and GSH (1 mM) added to Nitro 2 (1 mM) after electrolysis. Controls were done but are not included. Spectrometer conditions: microwave frequency 9.68 GHz microwave power 20 mW, modulation amplitude 0.4 G, scan rate 0.83 G/s, time constant 0.25 s number scans: 10.

This experimental evidence supports the idea that the trypanocidal effect of Nitro 1 occurs through a mechanism that does not involve oxygen radical generation. This evident mechanistic difference between Nitro 1 and Nitro 2 toxicity on *T. cruzi* is in agreement with the biological studies presented in Table III. These experiments, analysed in conjunction with the previous tables, strongly suggest that the antichagasic activity observed for Nitro 1 occurs though mechanisms involving inhibition of protozoal respiration. On the other hand, for Nitro 2 the main mechanism underlying its toxicity seems to be the production of oxidative stress state as a result of the extensive redox cycling Nitro 2 undergoes.

THEORETICAL CALCULATIONS

All internal coordinates for STO 3-21G *ab initio* calculations of both electron-paired and anion radical forms were completely optimised. In both above-mentioned structures the extended conformations for the side chain are the most stable. Furthermore, in all molecules the Nitro group lies in the plane of the ring for both neutral and anion radical forms.

The examination of the MO coefficients indicated that the SOMOs of the anion radical forms have antibonding pz characteristics and are mainly localized on the Nitro group. However, the unpaired electron was partially localised on the side chain.

In order to obtain the theoretical hyperfine constants, INDO calculations were performed using

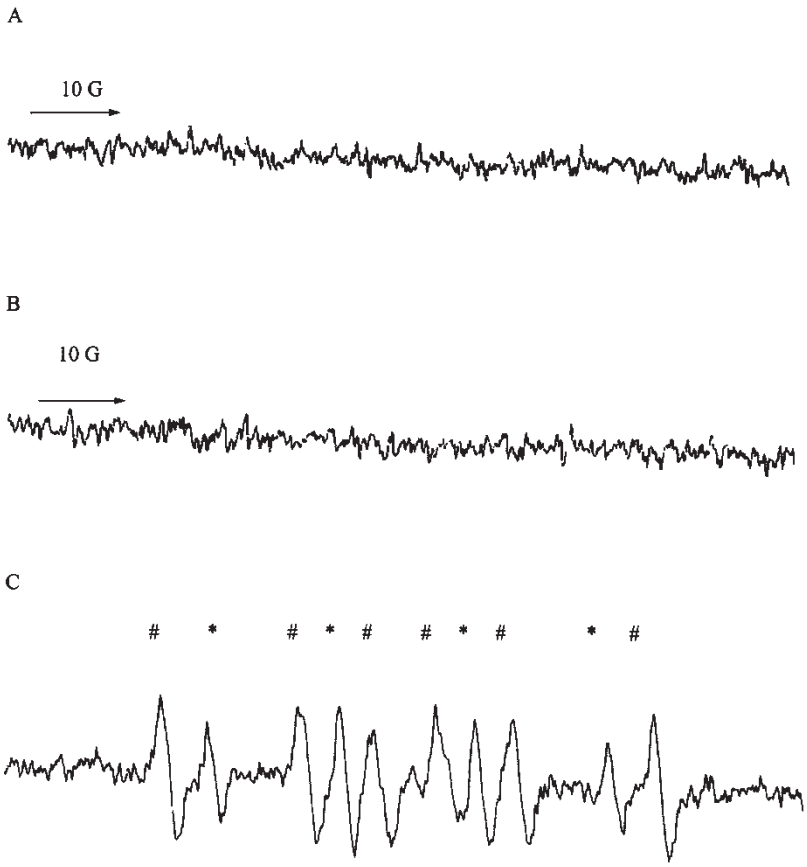

FIGURE 5 ESR spectra of DMPO-OH· and DMPO-nitro 2 radical adducts obtained with *T. cruzi* extracts. The ESR spectra were observed 10 min after incubation at 37°C with *T. cruzi* microsomal fraction (4 mg protein/mL), NADPH (1 mM), EDTA (1 mM), in phophate buffer (20 mM), pH 7,4 and (A) acetonitrile (10 v/v) and DMPO (100 mM), (B) Nitro 2 (1 mM in acetonitrile 10 v/v) and (C) Nitro 2 (1 mM in acetonitrile 10 v/v) and DMPO (100 mM) (DMPO-OH adduct (*): $a_N = a_H = 14.78$ G; DMPO-Nitro 2 adduct (#): $a_N = 15.21$ G, $a_H = 23.48$ G. Spectrometer conditions: microwave frequency 9.68 GHz microwave power 20 mW, modulation amplitude 0.4 G, scan rate 0.83 G/s, time constant 0.25 s number scans: 10.

the geometries obtained by STO-3-21G *ab initio* calculations. Table II shows both the experimental and calculated hyperfine constants. Comparison of these results shows agreement with the assignment of the hyperfine constants.

CONCLUDING REMARKS

The nitrofuran derivatives studied showed comparable voltammetric behaviours in DMSO. The first wave corresponded to a reversible one-electron transfer in which the anion radicals were formed. Both nitrofurans studies showed smaller $E_{1/2}$ than Nifurtimox. Furthermore, the reduction potentials of these nitro compounds correlated well with the experimental values estimated from IC_{kc50}. The ESR spectra of the anion radicals for Nitro 1 and 2 presented very good resolution. The hyperfine splittings in these spectra indicated that the electron delocalisation involved the side chain. The second peak was attributed to the production of the

TABLE III Effect of nitrtofuran derivatives upon culture growth and oxygen uptake in *Trypanosoma cruzi* epimastigotes

Nitrofuran derivative	IC_{kc50} (μM)*	nmol of drug/mg protein†	Respiration‡,¶	Oxygen redox cycling‡,¶§
Control	–		31.5 ± 1.7 (100%)	2.1 ± 0.5 (100%)
Nifurtimox	8.62 ± 0.2§	229	40.0 ± 1.0 (127%)	4.0 ± 1.5 (190%)
Nitro 1	5.21 ± 0.18	139	9.8 ± 1.0 (36%)	1.9 ± 0.7 (91%)
Nitro 2	2.83 ± 0.10	75	36.2 ± 1.0 (115%)	5.8 ± 1.0 (276%)

Values are expressed as mean ± SD of three independent experiments. See Materials and Methods section for details. * IC_{kc50} correspond to the micromolar nitrofuran derivative concentrations needed to reduce culture growth constant by 50%. † nmol of drug per mg of parasite protein used in culture growth (*) and respiration experiments (‡). ‡ Final drug concentrations used correspond to the IC_{kc50} equivalent concentrations as defined in Materials and Methods section. ¶ Respiration and oxygen uptake values are expressed as nanoatoms-gram of oxygen/min/mg protein. § Sodium cyanide (20μM) was added as well as the respective drug at the IC_{kc50} equivalent concentration.

hydroxylamine derivative. The third and fourth peaks (in Nitro 1) could correspond to a reductive process of the carbonyl group on the side chain. Also, from our study it has been demonstrated that nitro radical anions electrochemically generated from Nitro 1 and 2 were scavenged by GSH.

The hyperfine constants obtained by INDO calculations are in agreement with the experimental ones.

Finally, biological studies and the ESR experiment with the *T. cruzi* system indicate that Nitro 1 and 2 possess different mechanisms of toxicity. While Nitro 1 may act by inhibition of the parasite's respiratory cycle; Nitro 2 seems to do so by production of oxidative stress by increasing the redox recycling of the molecule.

Acknowledgements

This investigation was supported by FONDECYT—Chile grants Nos.1000834, 1020095 and 1020141.

References

[1] Schofield, C.J. (1985) "Control of Chagas' disease vectors", *Br. Med. Bull.* **41**, 187, http://www.who.int/whr/2001.

[2] Cerecetto, H. and González, M. (2002) "Chemotherapy of chagas' disease: status and new developments", *Curr. Topics Med. Chem.* **2**, 1185.

[3] Docampo, R. and Stoppani, A.O.M. (1980) "Generation of oxygen-reduction derivates induced by nifurtimox and other nitrocompounds in *Trypanosoma cruzi*", *Medicina* **40**(Suppl. 1), 10.

[4] Docampo, R. and Moreno, S.N.J. (1984) "Free radical intermediates in the trypanocidal action of drugs and phagocytic cells", In: Pryor, W.A., ed, *Free radicals in Biology* (Academic Press, New York) Vol **VI**, pp 243–288.

[5] Docampo, R. and Moreno, S.N.J. (1984) "Free radical intermediates in the trypanocidal action of drugs and phagocytic cells", In: Bors, W., ed, *Oxygen Radicals in Chemistry and Biology*, pp 749–751.

[6] Docampo, R., Moreno, S.N.J., Stoppani, A.O.M., Leon, W., Cruz, F.S., Villalta, F. and Muniz, R.P.A. (1981) "Mechanism of nifurtimox toxicity in different forms of *Trypanosoma cruzi*", *Biol. Biochem. Pharmacol.* **30**, 1947.

[7] Tracy, J.M. and Webster, L.T. (2001) "Drugs used in the chemotherapy of protozoal infections: amebiasis, trichomoniasis, trypanosomiasis, leishmaniasis, and other protozoal infections", In: Hardman, J.G., Limbird, L.E. and Gilman, A.G., eds, Goodman and Gilman's "The Pharmacological Basis of Therapeutics" (Mc Graw-Hill, New York), pp 1097–1120.

[8] Cerecetto, H., Mester, B., Onetto, S., Seoane, G., González, M. and Zinola, Z. (1992) "Formal potential of new analogues of nifurtimox: relationship to activity", *Farmaco* **47**(9), 1207.

[9] Cerecetto, H., Di Maio, J., Ibarruri, G., Seoane, G., Denicola, A., Peluffo, G., Quijano, C. and Paulino, M. (1998) "Synthesis and anti-trypanosomal activity of novel 5-nitro-2-furaldehyde and 5-nitrothiophene-2-carboxaldehyde semicarbazone derivatives", *Farmaco* **53**, 89.

[10] Di Maio, R., Cerecetto, H., Seoane, G., Ochoa, C., Arán, V.J., Pérez, E., Gómez, A., Muelas, S. and Martínez, A.R. (1999) "Synthesis and antichagasic properties of new 1,2,6-thiadiazin-3,5-dione-1,1-dioxides and related compounds", *Arzneimittel-Forsch. Drug. Res.* **49**, 759.

[11] Cerecetto, H., Di Maio, R., González, M., Risso, M., Sagrera, G., Seoane, G., Denicola, A., Peluffo, G., Quijano, C., Basombrío, M.A., Stoppani, A.O.M., Paulino, M. and Olea-Azar, C. (2000) "Synthesis and antitrypanosomal evaluation of E-isomer of 5-nitro-2-furaldehyde and 5-nitrothiophene-2-carboxaldehyde semicarbazone derivatives. Structure-activity relationships", *Eur. J. Med. Chem.* **35**, 343.

[12] Muelas, S., Di Maio, R., Cerecetto, H., Seoane, G., Ochoa, C., Escario, J.A. and Gómez-Barrio, A. (2001) "New thiadiazine derivatives with activity against Trypanosoma cruzi amastigote", *Folia Parasit.* **48**, 105.

[13] Martínez-Merino, V. and Cerecetto, H. (2001) "CoMFA-SIMCA model antichagasic nitrofurazone derivatives", *Bioorg. Med. Chem.* **9**, 1025.

[14] Paulino, M., Iribarne, F., Hansz, M., Vega, M., Seoane, G., Cerecetto, H., Di Maio, R., Caracelli, I., Zukerman-Schpector, J., Olea, C., Stoppani, A.O.M. and Tapia, O. (2002) "Computer assisted design of potentially active anti-trypanosomal compounds", *J. Mol. Struct. Theochem.* **584**, 95.

[15] Bouteille, B., Marie-Daragon, A., Chauvière, G., De Albuquerque, C., Enanga, B., Darde, M.L., Vallat, M., Périé, J. and Dumas, M. (1995) "Effect of megazol in *Trypanosoma brucei brucei* acute and subacute infection in Swiss mice", *Acta Trop.* **60**, 7.

[16] Enanga, B., Keita, M., Chauvière, G., Dumas, M. and Bouteille, B. (1998) "Megazol combined with suramin: a chemotherapy regimen which reversed the CNS pathology in a model of human African trypanosomiasis in mice", *Trop. Med. Int. Health* **3**, 736.

[17] Viodé, C., Bettache, N., Narimantas, C., Krauth-Siegel, R.L., Chauvière, G., Bakalara, N. and Périé, J. (1999) "Enzymatic reduction studies of nitroheterocycles", *Biochem. Pharmacol.* **57**, 549.

[18] Goijman, S.G. and Stoppani, A.O.M. (1984) "Oxygen radical and macromolecule turnover in *Trypanosoma Cruzi*", In: Rotilio, G. and Bannister, J.V., eds, *Oxidative Damage and Related Enzymes* (Harwood Academic Publishers, London, New York), pp 216–221.

[19] Olea-Azar, C., Atria, A.M., Mendizábal, F., Di Maio, R., Seoane, G. and Cerecetto, H. (1998) "Cyclic voltammetry and electron spin resonance studies of some analogues of Nifurtimox", *Spectrosc. Lett.* **31**, 99.

[20] Olea-Azar, C., Atria, A.M., Di Maio, R., Seoane, G. and Cerecetto, H. (1998) "Electron spin resonance and cyclic voltammetry studies of nitrofurane and nitrothiophene analogues of Nifurtimox", *Spectrosc. Lett.* **31**, 849.

[21] Rajagoplan, S. and Raman, P. (1955), *Org. Synth. Collect.* Vol. **3**, John Wiley and Sons, 425–427.

[22] Maya, J.D., Repetto, Y., Agosin, M., Ojeda, J.M., Tellez, R., Gaule, C. and Morello, A. (1997) "Effects of nifurtimox and benznidazole upon glutathione and trypanothione in epimastigote, trypomastigote, and amastigote forms of Trypanosoma cruzi", *Mol. Biochem. Parasitol.* **86**, 101.

[23] Maya, J.D., Morello, A., Repetto, Y., Rodríguez, A., Puebla, P., Caballero, E., Medarde, Núñez-Vergara, L.J., Squella, J.A., Ortiz, M.E., Fuentealba, J. and San Feliciano, A. (2001) "Novel antichagasic agents of the oxazolo(thiazolo)pyridine type. Relation between redox potential, lipophilicity, parasite culture growth and respiration inhibition", *Exp. Parasitol.* **99**, 1.

[24] Letelier, M.E., Rodriguez, E., Wallace, A., Lorca, M., Repetto, Y., Morello, A. and Aldunate, J. (1990) "*Trypanosoma cruzi*: a possible control of transfusion induced Chagas disease by phenolic antioxidants", *J. Exp. Parasitol.* **71**, 357.

[25] Maya, J.D., Bollo, S., Nunez-Vergara, L.J., Squella, J.A., Repetto, Y., Morello, A., Perie, J. and Chauviere, G. (2003) "*Trypanosoma cruzi*: effect and mode of action of nitroimidazole and nitrofuran derivatives", *Biochem. Pharmacol.* **65**, 999.

[26] Risch, M.J., Trucks, G.W., Schegel, H.B., Gill, P.N.W. Johnson, B.G., Robb, M.A., Cheeseman, J.R., Keith, K.T., Petersson, G.A., Montgomery, J.A., Raghavachari, K., Al-Laham, M.A., Zakrzewski, V.G., Ortiz, J.V., Foresman, J.B., Cioslowski, J., Stefanov, B.B., Nanayakkara, A., Challacombe, M., Peng, C.Y., Ayala, P.Y., Chen, W., Wong, M.W., Andres, J.L., Reploge, E.S., Gomperts, R., Martin, R.L., Fox, D.J., Binkley, J.S., Defrees, D.J., Baker, J., Stewart, J.P., Head-Gordon, M., Gonzalez, C. and People, J.A. (1998) Gaussian '98, Rev. A.7, Inc, Pittsburgh, PA.

[27] Baerendes, E.J., Allis, D.E. and Ros, P. (1990) "Self consistent molecular Hartree-Fock-Slater calculations. The computational procedure", *Chem. Phys.* **2**, 41.

[28] Vosko, S.H. and Wilk, L. (1983) "Accurate spin-dependent electron liquid correlation enrgies for local spin density calculations a critical analysis", *J. Phys.* **B16**, 3687.
[29] Stoyanovsky, D.A., Goldman, R., Jonnalagadda, S.S., Day, B.W., Claycamp, H.G. and Kagan, V.E. (1996) "Detection and characterization of the electron paramagnetic resonance-silent glutathionyl-5,5-dimethyl-1-pyrroline N-oxide adduct derived from redox cycling of phenoxyl radicals in model system and HL-60 cells", *Arch. Biochem. Biophys.* **330**, 3.
[30] Lai, C., Grover, T.A. and Piette, L.H. (1979) "Hydroxyl radical production in a purified NADPH-cytochrome C (P450) reductase system", *Arch. Biochem. Biophys.* **193**, 373.
[31] Moreno, S.N.J., Schreiber, J. and Mason, R.P. (1986) "Nitrobenzyl radical metabolites from microsomal reduction of nitrobenzyl chlorides", *J. Biol. Chem.* **261**, 7811.